Astron. Astrophys. 312, 879–896 (1996)

ASTRONOMY AND ASTROPHYSICS

Jet-like structures in β Lyrae

Results of optical interferometry, spectroscopy and photometry*

P. Harmanec[1], F. Morand[2], D. Bonneau[2], Y. Jiang[3], S. Yang[4], E.F. Guinan[5], D.S. Hall[6], D. Mourard[2], P. Hadrava[1], H. Božić[7], C. Sterken[8], I. Tallon-Bosc[9], G.A.H. Walker[3], G.P. McCook[5], F. Vakili[2], Ph. Stee[2], and J.M. Le Contel[10]**

[1] Astronomical Institute, Academy of Sciences of the Czech Republic, 251 65 Ondřejov, Czech Republic (hec@sunstel.asu.cas.cz, had@sunstel.asu.cas.cz)
[2] Observatoire de la Côte d'Azur, Département FRESNEL, CNRS URA 1361, St Vallier de Thiey, France (bonneau@ocar01.obs-azur.fr, morand@ocar01.obs-azur.fr, mourard@gi2t.obs-azur.fr, stee@altair.obs-azur.fr, vakili@rigel.obs-azur.fr)
[3] Department of Geophysics and Astronomy, University of British Columbia, 129-2219 Main Mall, Vancouver, B.C., V6T 1Z4 Canada (walker@astro.ubc.ca)
[4] Department of Physics and Astronomy, University of Victoria, P.O. Box 3055, Victoria, B.C., V8W 3P6 Canada (yang@uvastro.phys.uvic.ca)
[5] Department of Astronomy and Astrophysics, Villanova University, Villanova, PA 19085, USA (guinan@ucis.vill.edu, astronomy@ucis.vill.edu)
[6] The Arthur J. Dyer Observatory, Vanderbilt University, Box 1803, Nashville, Tennessee 37235, USA (hallxxds@ctrvax.vanderbilt.edu)
[7] Hvar Observatory, Faculty of Geodesy, Zagreb University, Kačićeva 26, 41000 Zagreb, Croatia (hrvoje.bozic@x400.srce.hr)
[8] Vrije Universiteit Brussel, Pleinlaan 2, 1050 Brussels, Belgium (csterken@vub.ac.be)
[9] U.M.R CNRS 142, Observatoire de Lyon, 9 avenue Charles Andre, F-69561 Saint-Genis Laval Cedex (bosc@image.univ-lyon1.fr)
[10] Observatoire de la Côte d'Azur, Département FRESNEL, CNRS URA 1361, B.P. 229, F-06034 Nice-Cedex 04, France (lecontel@rameau.obs-nice.fr)

Received 19 October 1995 / Accepted 13 February 1996

Abstract. A preliminary analysis of an extensive collection of interferometric, spectroscopic and photometric observations of the bright Be star β Lyr lead to the following main conclusions:

(1) The bulk of the Hα and He I 6678 emission seems to originate in jets of material perpendicular to the orbital plane of the binary. The jets are associated with the more massive component of the binary (star 1) and probably emanate from the 'hot spot' in the disk, i.e. the region of interaction of the gas stream flowing from the Roche-lobe filling B6-8II component (star 2) toward star 1. Some contribution to the emission also comes from a region located between the two stars (the gas stream and the 'hot spot') and from the 'pseudoatmosphere' of the accretion disk around star 1.

(2) The 282-d cyclic variation of the light curve of β Lyr is confirmed on the basis of 2852 homogenized V-band observations covering an interval of 36 yrs. We find, however, that the amplitude and phase of these variations vary with the orbital phase: the long-term modulation of the light curve almost disappears near orbital phases $0^P.25$ and $0^P.50$ (elongation and secondary eclipse).

(3) Pronounced line-profile variations of the Hα and He I 6678 lines on a time scale *shorter than one orbital period* were clearly detected. They may be periodic, with a period near $4^d.70 - 4^d.75$, and this periodicity may be related to the 282-d change via the orbital period.

Key words: stars: emission-line, Be – binaries: eclipsing – stars: individual: β Lyr – techniques: interferometric

1. Introduction

The second brightest star of the summer constellation Lyra, β Lyr, has been challenging astronomers for the past 200 years. A good and detailed review of the existing studies of β Lyr was published by Sahade (1980) and later extended by Plavec (1985). Some new developments and facts, directly related to the problems discussed here, are mentioned below.

β Lyr (10 Lyr, HR 7106, HD 174638, BD+33°3223, ADS 11745A) is the brightest member (component A) of an optical system of six stars and a 12.9-d spectroscopic and eclipsing binary with ample evidence of circumstellar matter within and around the system. The binary is at a distance of 370 pc from us (Dobias & Plavec 1985). According to current ideas, the β Lyr binary consists of the following two stars: (1) the more massive

Send offprint requests to: P. Harmanec

* Tables 2 and 4 are only available in electronic form at the CDS via anonymous ftp 130.79.128.5

** Belgian Fund for Scientific Research (NFWO)

star 1 (probably of an early-B spectral type) which is completely (or almost completely) hidden from view by a thick (presumably accretion) disk, and (2) a B6-8II companion (*star 2*) which is the brighter of the two in the optical region. Star 2 is brighter because of its large radius and because the light of star 1 is shielded by the circumstellar disk and re-radiated from the orbital plane. The binary orbit is very nearly circular and the primary eclipse of star 2 by star 1 and its disk is about $0^m.9$ deep in the visual; the secondary eclipse is $0^m.5$ deep. Due to combined effects of the ellipticity of star 2 and the presence of a thick disk, the light curve has no flat portions. Only the absorption lines of star 2 are visible in the spectrum and can be used to determine the radial-velocity (RV hereafter) curve. The orbital period has been growing at a rate of 19 s per year.

Wilson (1974) argued that – apart from occasional disturbances near the centres of the light minima – light variation of β Lyr is reasonably consistent and symmetric, with only infrequent departures greater than a few hundreds of a magnitude. He therefore concluded that the light-curve modelling should provide reliable information about the radii and relative luminosities of both bodies. He also argued that the disk around star 1 is massive (of the order of a solar mass), modelled it as a very flattened ellipsoid and presented the first detailed solution of the optical light curves. He indeed obtained some good fits and showed quite convincingly how the disk can redistribute the radiation of star 1 away from the orbital plane to account for the apparent 'underluminosity' of star 1.

Hubeny & Plavec (1991) presented a different quantitative model of the disk, assuming explicitly that the disk is *an accretion disk* and treating its vertical structure self-consistently. In contrast to Wilson's model, the disk proposed by Hubeny & Plavec has a negligibly small mass and is in the form of a normal Keplerian disk bounded from outside by a half-torus. Its 'height' (i.e thickness in the direction perpendicular to the equatorial plane) grows with the distance from the central star. Comparing their model with various data and using geometrical constrains, Hubeny & Plavec concluded that the disk has a radius of about 25 $R_\odot$ and height of about 6 $R_\odot$.

Guinan (1989) analyzed a long series of photoelectric observations of β Lyr and showed that its light curve *is not* secularly stable but varies in shape and amplitude (including the light maxima) with an apparent cycle of about (275 $\pm$25) d. This conclusion was reinforced in a recent study by Van Hamme et al. (1995) who reported the presence of periodic long-term variations of the light curve of β Lyr in several long data sets spanning 150 years and derived an improved period of $283^d.4$.

Batten & Sahade (1973) obtained Hα photographic spectra and concluded that the Hα emission consists of a broad and a narrow component. They argued that the narrow component shows little or no RV changes with the phase of the orbital period while the broad component moves in antiphase with respect to the RV curve of star 2. They also demonstrated the presence of secular changes in the emission strength. Soon thereafter, Kříž (1974) measured RV of the emission wings of Hα in the photographic spectra, showed that it was some 90° out of phase with respect to the RV curve of star 2 and pointed out that it was reminiscent of the so-called S-wave emission known for some cataclysmic binaries. Burnashev & Skulskij (1980) obtained flux-calibrated narrow-band Hα photometry of β Lyr and argued that the Hα flux varies with a quasi-period of $1^d.848$, i.e. 1/7 of the orbital period. Alekseev & Skulskij (1989) carried out fast scanning of the Hα line of β Lyr, confirmed the presence of very broad wings of the line at elongations and reported the presence of very rapid variations of the Hα emission on timescales from seconds to several tenths of minutes. They noted that these variations were the most pronounced at orbital phase $0^P.49$. They attributed this to effects due to the impact of the gas stream from star 2 to 1. Skulskij & Malkov (1992) and Skulskij (1993a) published RVs from CCD spectra of Hα. Their results show that the whole Hα emission moves approximately, but not exactly, in antiphase to the orbital motion of star 2.

Harmanec (1990) showed that reasonable component masses can be obtained on the assumption that star 2 exactly fills its Roche lobe and corotates with the binary. He estimated the mass ranges 13–15 $M_\odot$ and 3–5 $M_\odot$ for stars 1 and 2, respectively.

Skulskij & Topilskaya (1991) and Skulskij (1992) reported the discovery of weak absorption lines of Si II 2 lines at $\lambda\lambda$ 6347 and 6371 Å which moved in exact antiphase with respect to the lines of star 2. They interpreted them as photospheric lines and concluded that star 1 is an A5III object. Harmanec (1992) reinterpreted these lines as *shell lines* formed in the outer part of the disk around star 1. Using the geometrical arguments based on observations of absorption lines, presumably originating in the outer parts of the disk around star 1 and alternatively projected against either star 1 or star 2, he derived independent estimates of the disk dimensions which were in good agreement with what Hubeny & Plavec (1991) found.

Mazzali et al. (1992) studied the UV spectra of β Lyr and concluded that stellar winds from both components are observed. From a detailed analysis of the wind properties, they showed that the wind from star 1 indeed corresponds to that of an early-B main-sequence object.

Mourard et al. (1992) reported the first observations of β Lyr with the large optical spectro-interferometer GI2T. They were able to show that the emission structure seen in the Hα line was partly resolved by them.

Harmanec & Scholz (1993) analyzed 1532 RVs covering one century of observations and derived a new, very accurate ephemeris for the binary. They showed that the orbit is circular within the limits of observational accuracy and also concluded that the secular change of the orbital elements does not contradict the idea of the large-scale mass transfer from star 2 toward star 1. Arguing that the Si II lines discovered by Skulskij define the orbit of star 1 they also derived new masses for both stars.

Hubeny & Plavec's model has been criticized by Wilson & Terrell (1992) who objected to their non-selfgravitating thick disk. This criticism was discussed in detail and answered by Hubeny et al. (1994) who also suggested future strategy for the research and pointed out any serious problems remaining in the current understanding of the β Lyr system.

De Greve & Linnell (1994) attempted to model the evolutionary history of β Lyr as a system undergoing mass exchange from star 2 toward star 1 and concluded that the system has evolved in a non-conservative way from an initial system of 9 $M_\odot$ and 7.65 $M_\odot$. During the evolution, a small fraction of mass but a large fraction of the angular momentum was lost from the system according to their model.

Variable intrinsic polarisation of the continuum light of β Lyr have been known for about 60 years. Broad-band polarimetric observations show the dependence on the colour and also a correlation with the orbital phase (Appenzeller and Hiltner 1967). Rudy (1979) used the phase-dependent changes of the continuum polarisation to the determination of the spatial orientation of the binary. Narrow-band polarimetric measurements indicate that the variation of the intrinsic polarisation is associated with the emission and absorption structures at the Hα and Hβ lines (McLean 1977).

β Lyr has also been known as a radio source at centimeter wavelengths. Jameson & King (1978) proposed to associate the radio source with the H II region producing the strong optical emission lines. Observations of β Lyr with the Very Large Array may be indicative of a time variability of the radio emission (Leone, Trigilio & Umana 1994), but not much work has yet been done along this line.

Finally, Berghöfer & Schmitt (1994) reported that two of the optical components of the multiple system β Lyr, β Lyr A and β Lyr B, were detected as X-ray sources by ROSAT.

Questions about the true geometrical structure of the components of circumstellar matter around β Lyr, secular stability of the light curve and of the accuracy of the basic physical elements of the binary are clearly important for the ultimate understanding of the system and its evolutionary stage. We therefore decided to observe β Lyr systematically with the GI2T interferometer at different orbital phases. A collaborative program of nearly simultaneous spectral and photometric observations was also set up. Numerous observations were carried out in June–August 1994, with some spectroscopy and photometry also secured sooner and later in 1994 and earlier.

Here, we report the first principal results. We stress that this first paper on combined results does not deal with all aspects of the problem. We want to demonstrate what the data show and interpret the result in a semi-quantitative way only. Problems like detailed modelling of line profiles are being postponed for future studies. Since reliable recovery of the RVs of the weaker pair of the Si II 2 lines discovered by Skulskij (clearly seen also in our spectra) requires a subtraction of stronger absorption lines of star 2 and also of the emission components of the lines, we postpone also their analysis for a future study. We also put aside a study of the satellite lines seen prior and after the primary mid-eclipse.

Table 1. Journal of spectroscopic observations

Source	Epoch covered (JD-2400000)	No. of spectra
Skulskij (1972)	39251.5–40556.3	44
Batten & Sahade (1973)	41151.9–41163.7	17
Flora & Hack (1975)	41151.4–41165.4	19
Skulskij & Malkov (1992)	46301.3–48168.3	24
Skulskij (1993a)	48379.5–48548.3	27
Ondřejov 2.0-m	48804.5–49504.5	30
Ondřejov 2.0-m	49523.4–49599.4	65
Ondřejov 2.0-m	49612.3–49630.3	4
DAO 1.22-m	49574.7–49582.0	191
DAO 1.22-m	49631.9–49674.6	40

2. Observations, initial reductions and ephemeris

2.1. Spectroscopy

Altogether, 330 electronic spectra in the red spectral region were secured at the Ondřejov and the Dominion Astrophysical Observatories.

The collection of spectra in Ondřejov started immediately after the successful installation of the Reticon 1872 RF/30 detector in the coudé focus of the 2.0-m reflector, in May 1992. Altogether, 99 usable spectra were secured. They all have a linear dispersion of 17 Å mm^{-1} and cover the spectral region from 6300 to 6700 Å.

Most of the DAO spectra were secured in long series during 9 consecutive nights in August 1994; the rest was obtained in October and November 1994. These spectra were obtained in the coudé focus of the 1.22-m telescope, cover the spectral region from 6100 to 6700 Å and have a linear dispersion of 10 Å mm^{-1}. They were all recorded with a thick Loral 4096 × 200 CCD device with 15 μm pixels.

When analyzing the RV variations of the Hα and He I 6678 lines of star 2, we also used the quantitative data from 3 and 6 Å mm^{-1} CCD spectra published by Skulskij & Malkov (1992) and Skulskij (1993a). Additionally, we consulted earlier photographic studies of the Hα and He I 6678 line profiles of β Lyr published by Skulskij (1972), Batten & Sahade (1973) and Flora & Hack (1975). The journal of spectroscopic observations used here is presented in Table 1.

All initial reductions of DAO spectra (the background subtraction and flatfielding of 2-D images and creation of 1-D spectra in FITS format) were carried out by YJ and SY using the reduction package IRAF. All remaining reduction of these, and a complete reduction of all Ondřejov spectra was carried out by PHar with the reduction software SPEFO written by the late Dr. Jiří Horn. The wavelength calibration of the spectra was defined by a polynomial fit to the thorium-argon comparison spectra, now in use at both observatories. Polynomials of either 3rd or 5th degree were used. The spectra were rectified interactively on the computer screen but the program ensured that the fiducial points defining the continuum were always placed at the

Table 3. Journal of photoelectric observations of β Lyr. The following comparison and check stars were alternatively used: γ Lyr = HR 7178, 8 Lyr = HR 7100, 9 Lyr = HR 7102, HD 172044 = HR 6997 and η Lyr AB = HR 7298. They are identified by their HR numbers in the columns 'comparison' and 'check' here. Mean rms errors per one observation of the corresponding check star are given in the last three columns for each data set. See comments appended to Table 4 for the details of observation and reduction

Site instr.	Epoch (HJD-2400000)	No.	Filters	Comp.	Check	rms V	rms B	rms U
34	36375.7–36396.8	575	UBV	6997	7102	$0^m.012$	$0^m.013$	$0^m.018$
40	40025.7–41227.6	239	UBV	7178	7298	$0^m.06$	$0^m.03$	$0^m.09$
41	41056.9–41283.5	121	UBV	7178	7298	$0^m.03$	$0^m.03$	$0^m.03$
42	41132.7–41149.7	9	UBV	7178	–	–	–	–
39	44127.3–45155.3	235	BV	6997	7102	–	–	–
15	45749.1–46036.6	100	UBV	7100	7102	–	–	–
36	45969.6–47512.5	540	y	7178	–	–	–	–
15	46981.0–49443.0	819	VRI	7178	7102	$0^m.017$	–	–
38	49208.7–49647.6	105	BV	6997	7102	$0^m.016$	$0^m.042$	–
1	49272.3–49561.4	39	UBV	7178	7102	$0^m.009$	$0^m.012$	$0^m.013$
17	49482.0–49545.8	34	BV	7178	7102	$0^m.004$	$0^m.004$	–
16	49482.8–49637.6	32	$UBVRI$	7178	–	–	–	–
37	49541.4–49625.4	19	V_1	7178	7102	$0^m.025$	–	–

Stations and instruments are denoted by the internal running numbers used in the Ondřejov data archives as follows: 1... Hvar 0.65-m Cassegrain, data secured by HB, for reduction see Harmanec et al. (1994); 15... Phoexix 10: 0.25-m APT, UBV data secured by Boyd et al. (1990); and VRI data secured by Guinan (1989); 16... Fairborn-Villanova Univ. 0.8-m APT, data secured by EFG and GPM; 17... Vanderbilt Univ.0.4-m APT, data secured by DSH; 34... Lick 0.56-m Tauchmann reflector, unrefrigerated 1P21 tube, Wood & Walker (1960), Wood (1973); 36... Villanova Univ. 0.38-m reflector, y data secured by Guinan (1989); 37... Jungfraujoch 0.76-m reflector, Geneva P1 photometer, data obtained by CS and JML; 38... San Angelo, Texas, 0.25-m Schmidt-Cassegrain reflector, Optec SSP-3 solid state photometer, Sonntag (1995); 39... Ankara University Observatory 0.30-m Maksutov and EMI6256S tube, Aslan et al. (1987); 40... Chagrin Falls, Ohio, 0.25-m Cassegrain, 1P21 tube, Lovell & Hall (1970, 1971), Landis et al. (1973); 41... East Point, Georgia, 0.20-m Newtonian reflector, 1P21 tube, Landis et al. (1973); 42... Dyer Observatory, 0.60-m Cassegrain, 1P21 tube, Landis et al. (1973);

same wavelengths. Radial velocities were measured through the comparison of the direct and reverse images of the line profiles on the computer screen. This procedure was essential for the measurements of various details in the complicated line profiles of β Lyr.

The velocity measurements are presented in detail in Table 2[1]. RVs of the emission wings of whole emission lines, V and R peaks of emissions and strongest absorption cores were measured for both the Hα and He I 6678 lines, respectively. The stellar RVs of star 2 (the B8 component), as defined by the lines of Si II 2 and several stronger Ne I and Al II lines are also presented there.

To keep the RV zero point of both spectrographs under control, we measured a selection of good atmospheric lines in all spectra and applied necessary corrections. We therefore treat the DAO and Ondřejov RVs as originating from one spectrograph in all analyses (after verifying that there is indeed no significant difference in the RV zero point between them after the corrections were applied). Table 2 contains the corrected velocities.

2.2. *Photometry*

New photoelectric observations were secured during 1994 at several stations: $UBVRI$ observations were obtained with the Fairborn-Villanova Automatic Photoelectric Telescope (APT hereafter) located on Mt.Hopkins, Arizona, UBV observations with the Vanderbilt APT, located at the same site, and at Hvar and V_1 observations (of the Geneva 7-colour system) at Jungfraujoch. γ Lyr served as the primary comparison in all cases.

We also used and analyzed extended photometric observations secured earlier by three of us, EFG, GPM and DSH with their collaborators and certain published sets of photoelectric data. Hardly any other celestial object could compete with β Lyr in the number of existing photoelectric observations. Naturally, we had to be selective in the data compilation for the purpose of this study. On the other hand, we wanted to investigate further the reported presence of light variations on timescales different from the orbital period using a large collection of data from a number of sources, independent in their quality. A natural choice was to compile and homogenize sets of observations with reasonably low internal errors which were obtained on — or could be easily transformed to — the Johnson UBV system. We do not claim our compilation is complete but it can certainly be considered a representative sample with its 2852 yellow observations spanning an interval of 36 years.

The journal of photoelectric observations is presented in Table 3 while the individual observations with detailed comments on the reduction of homogenization of individual data sets can be found in Table 4.[1]

[1] Tables 2 and 4 are only available in electronic form: see the Editorial in A& AS 103, No.1 (1994)

Table 5. Stars which were alternatively used as comparisons in photoelectric observations of β Lyr and their UBV magnitudes adopted here

Star	HR	HD	Sp.	V	$B-V$	$U-B$
HR 6997	6997	172044	B8II	$5^m.423$	$-0^m.094$	$-0^m.518$
8 ν^1 Lyr	7100	174585	B3IV	$5^m.929$	$-0^m.142$	$-0^m.715$
9 ν^2 Lyr	7102	174602	A3V	$5^m.242$	$0^m.097$	$0^m.093$
14 γ Lyr	7178	176437	B9III	$3^m.253$	$-0^m.071$	$-0^m.052$

We created an archive of differential observations (containing the magnitude differences *var − comp* and *check − comp* with the HD numbers of respective comparison stars) which were further organized, sorted and retrieved with the help of program VYPAR — see Harmanec & Horn (1995). That is why the individual stations are identified by the running numbers according to the system adopted at the Ondřejov archives.

Since different observers used different comparison stars, our 1994 observations also served to establish observations of all of these comparisons relative to γ Lyr. Special care was devoted to this task at Hvar. We adopted the mean all-sky standardized UBV values, based on several years of Hvar observations, for γ Lyr (c.f. Harmanec, Horn and Juza 1994) while the adopted UBV magnitudes of all other comparisons are the mean differential values relative to γ Lyr, also derived at Hvar. The adopted magnitudes of all comparisons, used for the homogenization of all data sets (see comments on individual sets appended to Table 4) are listed in Table 5. The degree of internal consistency of this procedure can be judged from an inspection of Table 6 where the adopted Hvar values are compared with the mean magnitudes of the same stars, derived differentially relative to the respective comparisons for which the values from Table 5 were adopted. It is seen that the agreement is satisfactory for our purpose, certainly much better than in previous similar studies based on combination of data from many observatories. (We confirm the suspicion of Wood & Walker (1960) that 8 Lyr may be slightly variable. The most probable time scale of the variations appears to be 14–15 d.) It seems justified, therefore, to homogenize the existing observations of β Lyr by adding the adopted values from Table 5 for respective comparisons to the standardized magnitude differences β Lyr – comparison. This is what we did.

We stress that in the following analyses of orbital and non-orbital variations we shall rely primarily on the observations through yellow filters. The reason is that the V magnitude is the easiest one to reproduce in different standard systems and it is also relatively little affected by the extinction errors (since the extinction in yellow is smaller than in blue or UV wavelengths). To a high degree of accuracy, the instrumental yellow magnitude can usually be transformed to the standard Johnson system via a linear relation

$$V = V_{\rm instrumental} + k(B-V),$$

Table 6. UBV values of 8 Lyr and 9 Lyr derived differentially relative to various comparison stars (denoted by their HR numbers in column "Comp.") for which the values of Table 5 were adopted

Star	V	$B-V$	$U-B$	Comp.	Station
8 Lyr	$5^m.929$	$-0^m.142$	$-0^m.715$	7178	Hvar
	$5^m.948$	$-0^m.152$	$-0^m.707$	6997	Lick
	$5^m.911$	–	–	7178	Jungfraujoch
9 Lyr	$5^m.242$	$0^m.097$	$0^m.093$	7178	Hvar
	$5^m.242$	$0^m.095$	$0^m.068$	6997	Lick
	$5^m.240$	–	–	7178	Villanova
	$5^m.236$	$0^m.072$	–	7178	Vanderbilt
	$5^m.235$	–	–	7178	Jungfraujoch
	$5^m.209$	$0^m.102$	–	6997	San Angelo

where the transformation coefficient k is smaller than 0.15 for most of photometers. Very fortunately, the $B-V$ colour difference between β Lyr and the primary comparison star γ Lyr is only about $0^m.05$ which means that the transformation errors should be smaller than $0^m.008$. Thanks to this circumstance, it is justified to create the standard V magnitude of β Lyr by adding any transformed yellow magnitude difference β Lyr – comparison to our adopted V magnitude of γ Lyr.

Another check on the accuracy of individual data sets is provided in Table 3 where the mean rms errors per 1 observation are given for the respective check stars.

2.3. *The ephemeris*

We used our stellar RVs and also RVs from recent electronic spectra published by Skulskij (1992, 1993b) to check how well the ephemeris by Harmanec & Scholz (1993) fits the recent data. The RV curve based on our RVs is shown in Fig. 1. It is seen that we achieved a very good phase coverage. An orbital solution for a circular orbit for these RVs gives

$K_2 = 185.6 \pm 0.3$ km s^{-1}, $\gamma = -16.8 \pm 0.3$ km s^{-1},

$T_{\rm prim.min.} = {\rm HJD}\ 2449559.9801 \pm 0.0043$.

The semi-amplitude is in excellent agreement with the results of Harmanec & Scholz (1993). The O-C of the epoch with respect to their ephemeris is $0^d.0234 = 0^P.0019$.

To check further on the exact phasing, we calculated local epochs for data subsets spanning no more than 45 d for all RVs used by Harmanec & Scholz (1993) as well as for the new RVs, carefully excluding subsets with unsatisfactory phase distribution. Computer code FOTEL (Hadrava 1990, 1995) was used for all orbital solutions presented here. A plot of the O-C deviations of these local epochs vs. phase of the ephemeris of Harmanec & Scholz (1993) exhibits some scatter (which is only marginally higher than the formal rms errors of the local epochs for most of the subsets) but no systematic trend is found. We also subjected these O-C deviations to a period analysis for periods longer than 100 days. No significant periodicity was detected.

Fig. 2 shows the V magnitude light curve based on data obtained over the same period in 1994 as the spectral and inter-

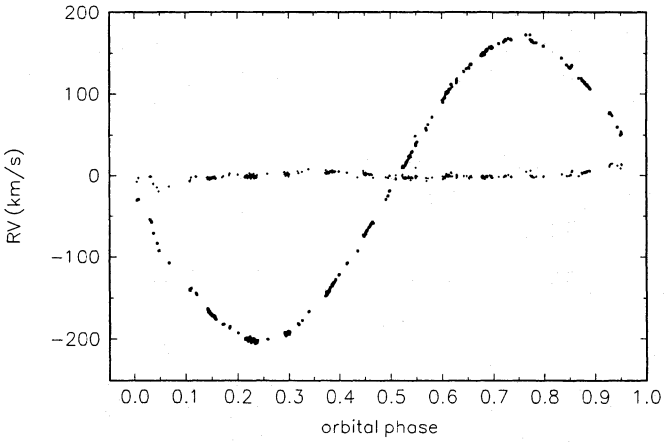

Fig. 1. Mean RVs of star 2 (B8 component) of β Lyr measured from the red Ondřejov and DAO electronic spectra vs. phase from the ephemeris by Harmanec & Scholz (1993). RVs are shown by filled circles, the O-C deviations from the orbital solution for circular orbit by pluses.

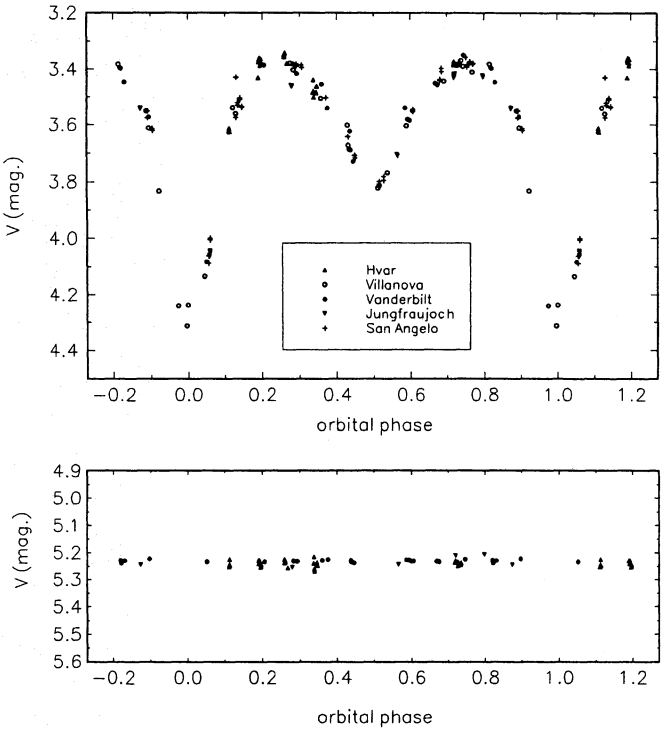

Fig. 2. The 1994 light curve of β Lyr (only data from JDs 2449500–700, i.e. from the period of 1994 interferometric and spectral observations) vs. phase from the ephemeris by Harmanec & Scholz (1993). Individual stations are denoted by different symbols. The data for the most frequently used check star, 9 Lyr, are also shown on the same scale.

ferometric data. It also shows a very good agreement with the ephemeris used.

We conclude that the use of the ephemeris by Harmanec & Scholz is fully justified for our purposes, any possible errors in exact phasing being certainly smaller than $0^{\rm p}.01$.

2.4. Interferometry

The observations reported here were carried out with the GI2T interferometer at the Plateau de Calern (for a detailed description, see Mourard et al. 1994a). All observations were carried out with a North–South baseline of 51 m and calibrated using observations of γ Lyr. Our planned strategy was to observe γ Lyr *always* prior to *and* after β Lyr but this was often not possible because of the unusually poor atmospheric conditions. The data were recorded at two wavelength bands 12nm wide centred on the Hα and He I 6678 lines (hereafter the Hα and He I 6678 channel, respectively). The position of the He line on the detector was close to the maximum sensitivity which at the same time prevented saturation of the much stronger Hα emission. The dispersed fringes were recorded with the CP40 photon counting camera (Blazit 1987). 20-ms exposures were used to freeze the atmospheric turbulence. Each record contains a sequence of short exposures secured during 1 to 3 minutes. All records were then inspected by DB, FM, DM, and IT-B and poor-quality data were omitted. The journal of usable interferometric observations is in Table 7.

The detailed data processing was described by Mourard et al. (1994b). After correction for the optical distortions of the detector (Thiebaut 1994), the data were first integrated to obtain an image of the stellar spectrum. For an analysis of the visibility function, both studied spectral channels were divided into four spectral bandpasses: one bandpass was centred on the whole emission line, another one on the violet emission peak, the third one on the red emission peak, and the last one was set at the continuum redward of the line. The choice of the boundary wavelengths of the bandpasses for each orbital phase was carried out on the basis of the RV information for the individual emission features obtained from the high-dispersion Ondřejov and DAO spectra. Fig. 3 is an example of the observed GI2T spectrum showing the position of the spectral bandpasses used for the interferometric analysis.

3. Interferometric results

3.1. Visibility calibration

To detect spectral or time variations in the angular size of the source, one has to calibrate the observed fringe visibilities measured for β Lyr (denoted by a suffix 'obs') to give calibrated ('cal') visibilities.

We used the star γ Lyr for this calibration. The angular diameter adopted for γ Lyr, $\theta = 0.742 \pm 0.097$ mas, was derived by Legett et al. (1986). They used the infrared flux method proposed by Blackwell & Shallis (1977). (The angular diameter seems to be in a reasonable agreement with the spectral type B9III, Strömgren photometry and measured parallax of the star.) Using the projected baseline on the sky, $B_{\rm p}$ = 50.1 m, and the central wavelength of 6600 Å, we derive the theoretical fringe visibility $V_{\rm th}^{\gamma{\rm Lyr}} = 0.915 \pm 0.025$. Then, for each night, we compute the calibrated visibility for β Lyr in every spectral band using the relation

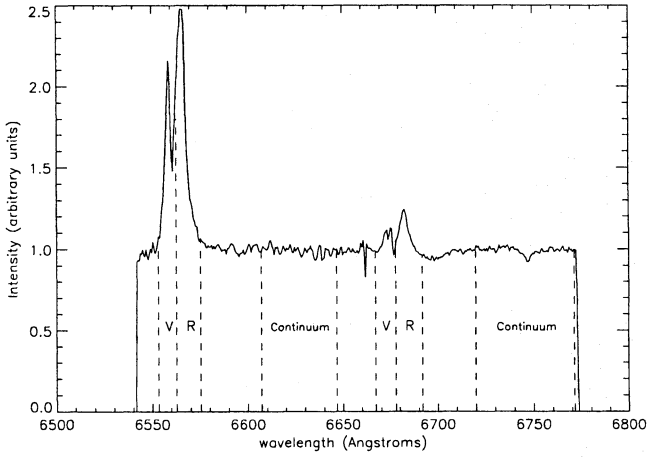

Fig. 3. The GI2T spectrum of β Lyr from the July 17 night showing the spectral bandpasses used: the violet emission peaks (V), red emission peaks (R), whole lines (V + R) and continua. The "narrow absorption line" feature close to λ6660 is an artefact due to the reconnection of the Hα and He I 6678 channels.

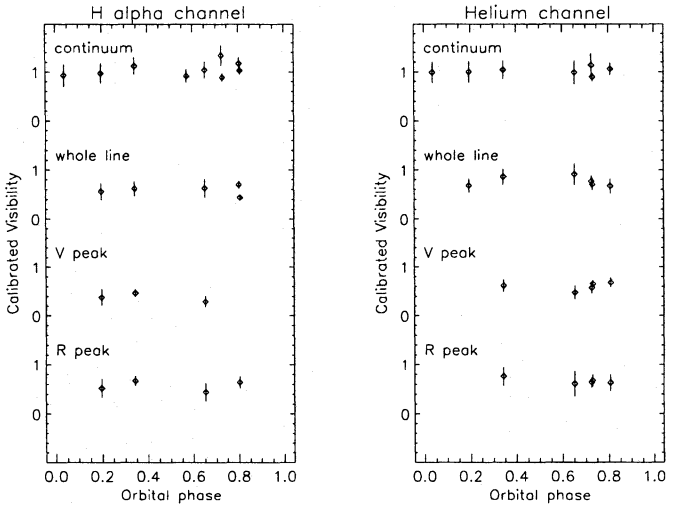

Fig. 4. The calibrated visibilities of β Lyr in the Hα (left) and He I 6678 (right) channels vs. orbital phase. From top to bottom: continuum, whole line, V and R emission peaks

Table 7. Journal of interferometric observations of β Lyr and γ Lyr. Heliocentric Julian dates (HJD) and orbital phases refer to the mean times of the data files recorded at each given night. The third column gives the number of records for β Lyr. The number of records for γ Lyr prior (p) and/or after (a) the observation of β Lyr are given in the last column.

HJD (JD-2400000)	Orb. phase	β Lyr	γ Lyr p - a
49541.5039	0.574	14	7 - 0
49543.4887	0.727	16	6 - 4
49544.4887	0.804	14	7 - 4
49547.4777	0.036	6	9 - 0
49551.4640	0.344	19	9 - 7
49555.4635	0.653	26	11 - 0
49568.4167	0.654	12	0 - 2
49569.4196	0.731	7	4 - 0
49570.4084	0.808	7	0 - 7
49588.3571	0.195	11	0 - 7
49601.3257	0.197	10	0 - 5

$$V_{\rm cal}^{\beta\ \rm Lyr} = V_{\rm obs}^{\beta\ \rm Lyr} \frac{V_{\rm th}^{\gamma\ \rm Lyr}}{V_{\rm obs}^{\gamma\ \rm Lyr}}.$$

3.2. Spectral continuum

The upper part of Fig. 4 presents the calibrated visibility of β Lyr for the continua in the Hα and He I 6678 channels. No obvious phase dependence of the continuum calibrated visibility is found but we note that the available observations are insufficient for that purpose, both in their number and their phase distribution.

The averaged calibrated visibilities of β Lyr in the two channels are $V_{\rm cal}^{\beta\ \rm Lyr} = 1.02 \pm 0.16$ and 1.00 ± 0.20, respectively. This means that the angular extension of the source of continuum radiation in β Lyr along the N-S direction is unresolved with the adopted baseline.

The analysis of the visibility in the continuum light indicates that the binary β Lyr (star 1 + accretion disk and star 2) is unresolved by GI2T with the maximum baseline currently in use, independently of the orbital phase. The estimated angular extension of the object based on the model of Hubeny & Plavec (1991) ($\sim$ 1.3 $\times$ 0.3 mas) implies that the orientation of the binary components at the maximum elongation must be close to the East-West direction otherwise it would be measurable with the GI2T North-South baseline. This result confirms the spatial orientation of the projection of the vector of the orbital angular momentum of β Lyr on the sky, $\theta = 160°$ counted from the North, given by Rudy (1979).

3.3. Hα and He I 6678 lines

The calibrated visibility in the Hα line (see the left panel of Fig. 4) is always smaller than 1.0 which means that the source of the Hα emission is more extended than the source of the continuum. This result is in accordance with an earlier finding by Mourard et al. (1992). Again, no evidence of phase-dependent changes was found from our limited data.

The calibrated visibilities of β Lyr through the V and R emission peaks indicate that the associated sources are also individually resolved. Perhaps the most unexpected result is, however, that the visibility of the violet peak is *always* smaller than that of the red one.

The calibrated visibility of the He I 6678 emission (see Fig. 4 right part) is smaller than 1.0, which means that the source of the He I emission is also more extended than the source of the continuum. Again, no significant variation of the visibility with the orbital phase was found.

Table 8. Mean calibrated visibility of β Lyr in the emission lines Hα and He I 6678

Spectral band	Hα	He I 6678
whole line	0.55 ± 0.13	0.76 ± 0.15
V peak	0.39 ± 0.12	0.62 ± 0.11
R peak	0.59 ± 0.15	0.66 ± 0.17

In contrast to the result for the Hα emission, the visibilities of the source in the V and R parts of the He I 6678 emission are equal.

Table 8 summarizes the mean calibrated visibilities for both of the lines studied.

The fact that the visibility of β Lyr in V and/or R peak appears to be smaller than the visibility in the whole line implies that the spectral lines are formed in (possibly quite localized) regions which are located elsewhere than the source(s) emitting the continuum light through the Hα line. The absence of any significant variation of the visibility with the orbital phase implies that the orientation of the resolved sources contributing to the emission of Hα and He I 6678 lines could be perpendicular to the orbital plane. This agrees with a recent analysis of UV line polarization by Nordsieck et al. (1995) which suggests bipolar flow or jets at a position angle of 162°.

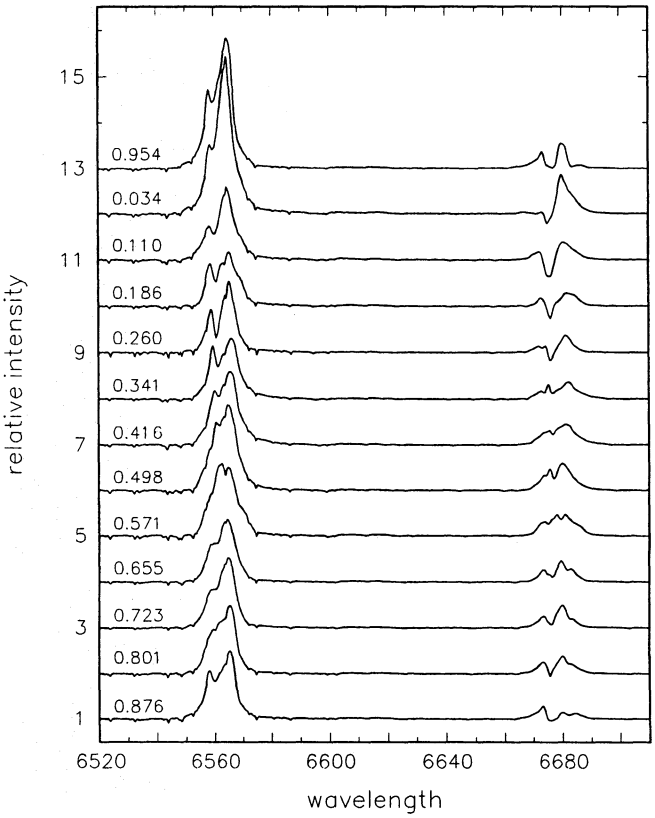

Fig. 5. Examples of the observed Reticon Hα and He I 6678 line profiles of β Lyr at various orbital phases, given for each spectrum

4. Orbital spectral and light variations

A representative selection of the Hα and He I 6678 line profiles from various orbital phases is shown in Fig. 5. It would not be wise to combine the Reticon and CCD spectra in this figure because of their different spectral dispersion and resolution. We had, therefore, to use Reticon spectra only since the CCD spectra do not cover all intervals of orbital phases. To illustrate the effects of the different resolution, we compare a Reticon and a CCD Hα spectrum, which were obtained within $0^d.3$ one after the other, in Fig. 6.

All spectra displayed in Fig. 5 come from orbital cycles 3195–3196, with the exception of the spectrum from phase 0.260, which is from an earlier cycle 3162. (For comparison, the interferometric observations cover cycles 3194 through 3199.) It is seen that the profiles are quite complex and their RV measurements are not straightforward. Correct RV measurements of the emission or absoption parts of the profile, for instance, should be carried out in the profiles from which the absorption profile of star 2, and then the emission profile were subtracted (or better say properly removed). However, this can only be carried out if we know the true shape and RV of each such contributor for each spectrum. This is not so at the moment. Clearly, one has to proceed in an iterative way to understand what is really going on. Here, we shall only deal with the first iteration of the process — description and preliminary analyses of the RV curves of several details in the profiles as measured *directly from them.*

4.1. Hα

Fig. 7 shows an enlargement of the bottom parts of the Hα profiles with the extended broad emission wings, first discussed by Batten & Sahade (1973). It is immediately seen that it is *always the red wing* which is the more extended, at all orbital phases. This leads us to conclude that this extended wing is *not* a part of the Hα profile but another feature, very likely *a blend of the emission components of the C II 2 doublet at 6578.0 and 6582.9 Å.* We note that there is also a weak broad emission line near 6611 Å which is probably due to the N II 6610.56 Å line, with possible contributions from S II lines at 6604.74 and 6611.04 Å. Note that the C II 2 and λ 6611 Å emissions stand out very clearly in a Reticon spectrum of P Cyg, which is also shown for comparison in Fig. 7. This strengthens our interpretation of the extended red wing of Hα. We, therefore, cannot fully support the conclusion by Batten & Sahade that there is a broad Hα emission from an envelope around star 1 and a narrower emission from a cloud around the whole system.

An inspection of Figs. 5 and 7 reveals that the Hα absorption from star 2 is almost completely masked by the strong Hα emission while the best defined detail in most of the profiles is the absorption core. It is strong, rather symmetric and sharp enough for accurate RV measurements everywhere with the exception of a phase interval of about $0^P.55$–$0^P.70$. Since RV measurements of this absorption core are also available from several earlier

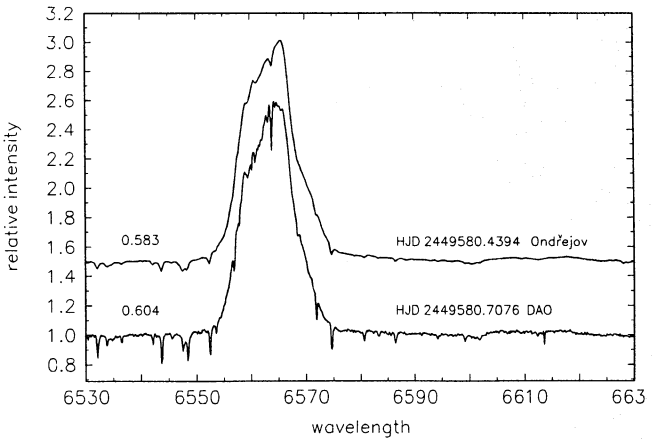

Fig. 6. Comparison of one Reticon and one CCD spectrum obtained shortly one after the other. Orbital phases are indicated

studies, we start the discussion of Hα velocities with the RVs of the absorption core. Then, individual measured parts of the emission are discussed.

4.1.1. Absorption core

Fig. 8 (top) shows the phase changes of the Hα absorption velocities in relation to the orbital motion of star 2. It is seen that the RV curve of the Hα absorption is sinusoidal but shifted by almost exactly $0^{P}.25$ with respect to that of star 2. In spite of some scatter (which is larger at phases where the absorption gets shallow), the RV curve of the Hα absorption shows a good secular stability (the data span an interval of about 10000 d). A formal circular orbital solution for all 302 Hα absorption RVs (with weights inversely proportional to dispersion) gives

$K_{abs.}$ = 45.97 $\pm$0.76 km s^{-1},
$T_{\min.RV}$ = HJD 2449559.499 $\pm$0.035,
$\gamma = -81.65 \pm 0.56$ km s^{-1},
rms of 1 observation of unit weight: 8.7 km s^{-1}.

This is a very notable result. It seems to imply that the bulk of the Hα absorption is formed in a localized region which *lies outside the line joining the two stars* and revolves around the centre of gravity of the binary. The phase of the epoch of minimum RV is $0^{P}.9647 \pm 0^{P}.0027$. Assuming an orbital inclination of $i = 83°$ (Hubeny & Plavec 1991) and using the well-known relation

$$r/R_{\odot} = (P\,v)/50.633,$$

where r denotes the radial distance from the centre of rotation, P the rotational period in days and v the linear orbital velocity, one finds that the distance of the region producing the Hα absorption from the centre of gravity is 11.84 $R_{\odot}$. Using the phase of RV minimum, one finds the position of the region in the coordinate system with the origin in the centre of star 1 and X axis defined by the line joining the centres of both stars as

X=8.06 $R_{\odot}$ and Y=11.55 $R_{\odot}$

if one adopts the basic physical elements of the system derived by Harmanec & Scholz (1993). Note that the coordinates of the centre of gravity are

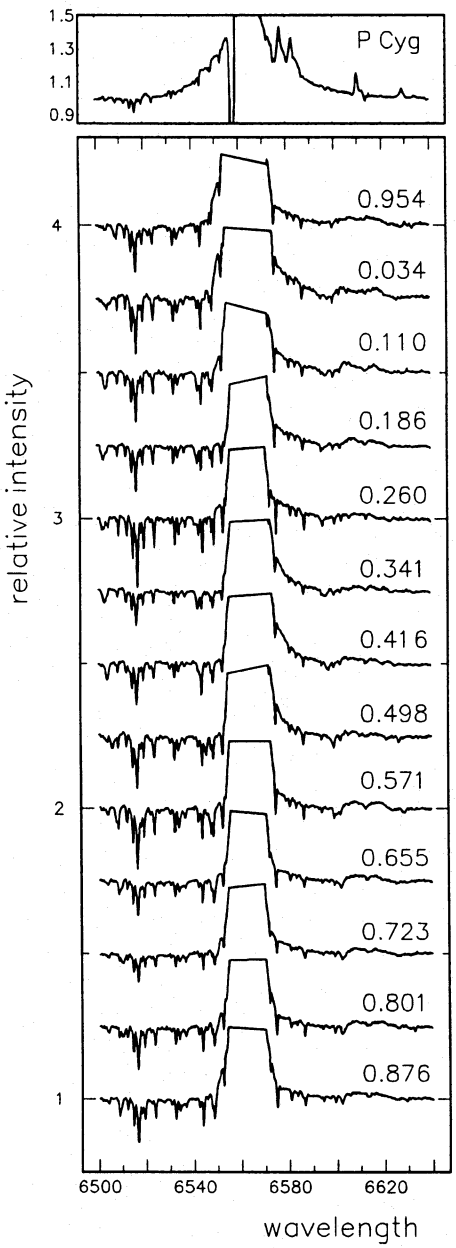

Fig. 7. Enlarged spectra in the neighbourhood of Hα , showing the character of the extended emission wings and also a weak broad emission feature at about 6611 Å. Corresponding orbital phases are given for each spectrum. Note that the upper parts of the Hα emission were artificially removed to increase the contrast of the bottom parts of the line profiles. For comparison, a Reticon spectrum of P Cyg is also shown

X=10.67 $R_{\odot}$ and Y=0 $R_{\odot}$.

4.1.2. Wings of the whole emission

Fig. 8 (bottom) is a phase plot of the RV of the emission wings of Hα, based on our data and on observations by Batten & Sahade (1973) (broad line), Skulskij & Malkov (1992) and Skulskij (1993a). The relatively large scatter reflects the problems with accurate settings mentioned earlier. Nevertheless, it is seen

that the Hα emission as a whole moves *almost* in anti-phase to star 2. A formal orbital solution gives

$K_{em.}$ = 31.9 ±1.9 km s^{-1},
$T_{\rm min.RV}$ = HJD 2449558.057 ±0.082,
γ = 6.0 ±0.9 km s^{-1},
rms of 1 observation of unit weight: 17.6 km s^{-1}.

One can note that the phase of RV minimum is $0^{\rm P}.853$ (instead of $0^{\rm P}.75$ for star 1). Using the same procedure as for the absorption core, one can estimate the coordinates of the "optical centre of gravity" of the emission line as

X = 4.12 R$_\odot$, Y = 4.97 R$_\odot$,

i.e. not far from the centre of star 1. The semiamplitude of the RV variation of the Hα emission is lower than that of star 1 as derived by Harmanec & Scholz (1993). However, the difference need not be real since the absolute value of the measured RV of Hα emission near both elongations is inevitably decreased by the blending effects of stellar–line absorption of star 2.

Ignoring the extended very broad red wing of the Hα emission (likely due to C II 2 emission blend), we also estimated the width of the emission profile at its edges. It corresponds to about ±630 km s^{-1}. If interpreted as dynamical broadening due to Keplerian rotation in the disk around star 1, it would give a radius of about 6.3 R$_\odot$ for the corresponding emitting region (on the assumption that the mass of star 1 is 13.2 M$_\odot$ which follows from the elements of Harmanec & Scholz 1993 for i = 83°). We note that this radius agrees well with the expected radius of star 1 hidden inside the disk.

One could also argue that the mean velocity of the Hα emission which is more positive than the systemic velocity of the binary is indicative of some net infall of gas toward star 1. We do not think such a suggestion can be defended seriously until one excludes the effects of line blending over the wavelength range of the broad Hα emission line.

4.1.3. V and R emission peaks

As it is seen already from Fig. 5, the positions of the V and R peaks of Hα are obviously affected by the RV and width variations of the absorption core, by (barely visible) blending due to the Hα absorption line of star 2 and by the RV variation of the whole emission line. The observed variation of the emission peaks is shown in Fig. 9. It is seen that the V peak follows a RV curve approximately in phase with the RV curve of the Hα absorption while the (usually stronger) R peak follows a double-wave curve. In our opinion, the observed behaviour is a direct consequence of the effects mentioned above and does not represent any great puzzle. In the first half of the orbital period (phases $0^{\rm P}.0$ to $0^{\rm P}.5$), the stronger R peak follows the RV curve of the whole emission but shifted for some 100 km s^{-1} to the red. In phases $0^{\rm P}.5$ to $0^{\rm P}.9$, the absorption line gets broader which makes the R-peak RV more positive and the V-peak RV more negative. The fact that the V-peak RV is more affected by the RV of the absorption core while the R peak mainly follows the RV curve of the whole emission is simply understood if one realizes that the absorption is blue-shifted all the time and does not affect both emission peaks in the same manner. We conclude that the RV variation of the emission peaks do not contain any new piece of evidence about the structure of the circumstellar matter.

4.2. He I 6678

As seen in Fig. 5, the He I 6678 line has much less intense emission components than Hα and is, therefore, much more affected by the absorption lines. RVs of all consistently identified observable features of apparent absorption and of emission wings are shown in Fig. 10, separately for the Reticon and CCD data. Orbital variation of various absorption components create an impression of three emission peaks in certain orbital phases. However, considering also the Hα results, we do not investigate the RV variations of any of these emission peaks. An absorption line of star 2 is clearly present in the He I 6678 line. We note, however, that its RV amplitude is inevitably distorted as the line falls into the steep wings of the He I 6678 emission. Besides the absorption analogous to that seen in Hα, another absorption is occasionally present which seems to vary roughly in antiphase to the principal one. One can also recognize satellite absorption lines seen prior and after the primary eclipse.

Considering the results for Hα, we restrict further discussion of the He I 6678 line to the RV behaviour of the absorption cores and emission wings.

4.2.1. He I 6678 absorption cores

A formal orbital solution for the principal He I 6678 absorption gives

$K_{abs.}$ = 41.4 ±0.9 km s^{-1},
$T_{\rm min.RV}$ = HJD 2449559.872 ±0.037,
γ = −84.19 ±0.59 km s^{-1},
rms of 1 observation of unit weight: 8.9 km s^{-1}.

This shows that this He I 6678 absorption originates in the same region as the Hα absorption and has the same expansion velocity.

We have no ready interpretation for the weaker second absorption seen in some spectra and postpone its study for a future investigation of the profiles from which some principal contributors (like star 2 absorption) will be properly removed.

4.2.2. He I 6678 emission wings

It is obvious from Fig. 5 that the accurate RV measurements of the wings of the He I 6678 emission are strongly hampered by the presence of various absorptions in the profiles. Not surprisingly, these RVs show a great deal of scatter. Yet, they seem to vary nearly in antiphase to the orbital RV curve of star 2, attaining minimum RV at phase $0^{\rm P}.80$. Very probably, also the He I 6678 emission originates from the same region as the principal contributor to the Hα emission.

4.3. Light changes

The 1994 orbital light curve in the V band has already been shown earlier (cf. Fig. 2). To interpret the Hα variations, we

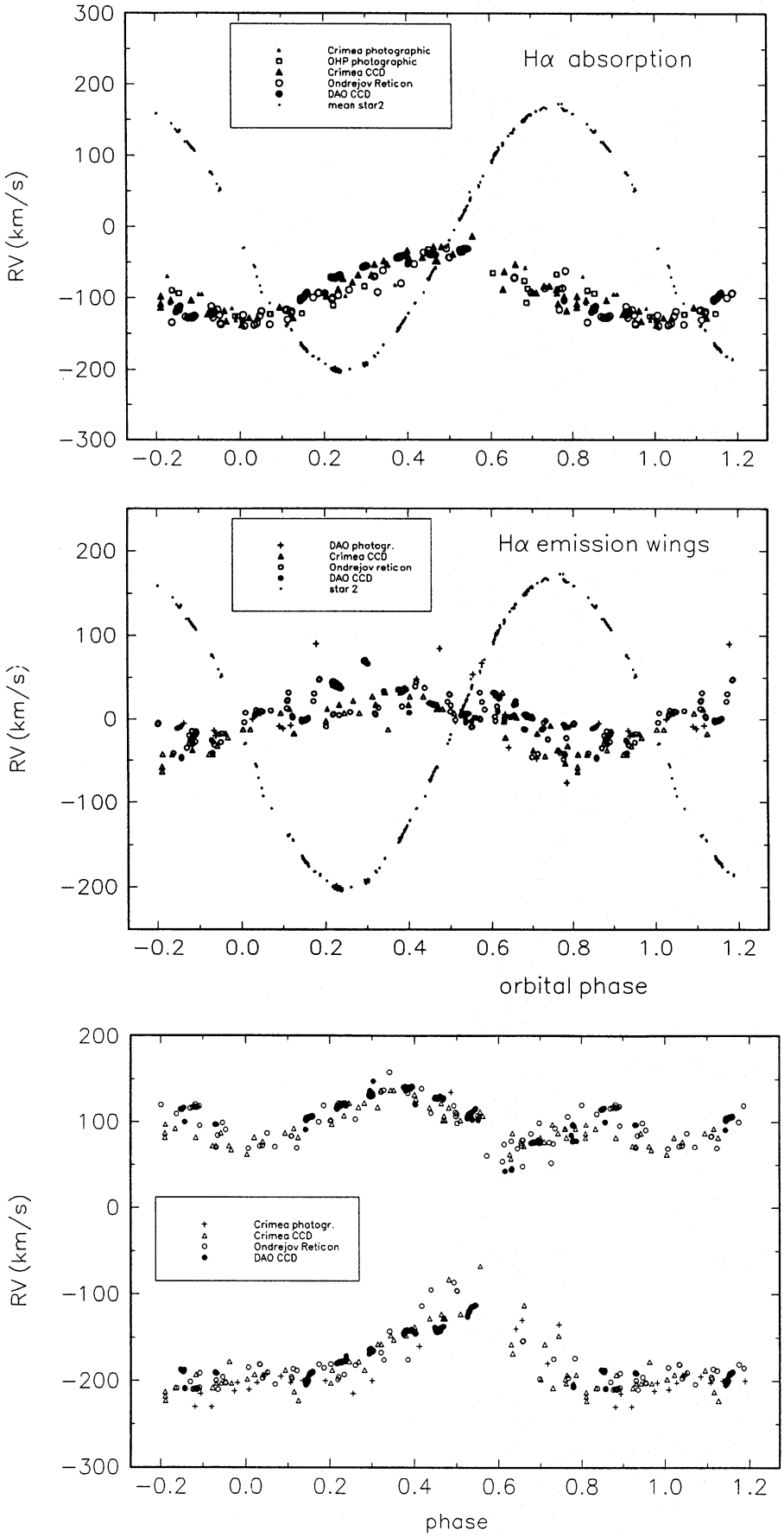

Fig. 8. *Top:* RV curves of the Hα and He I 6678 absorption cores, as measured by us and by several previous investigators, versus orbital phase. The RV curve of star 2 is also shown for reference. *Bottom:* RV curve of the emission wings of Hα, as measured by us and by several previous investigators, versus orbital phase. The RV curve of star 2 is also shown for the reference.

Fig. 9. RV curve of the Hα R and V emission peaks, as measured by us and several previous investigators, versus orbital phase

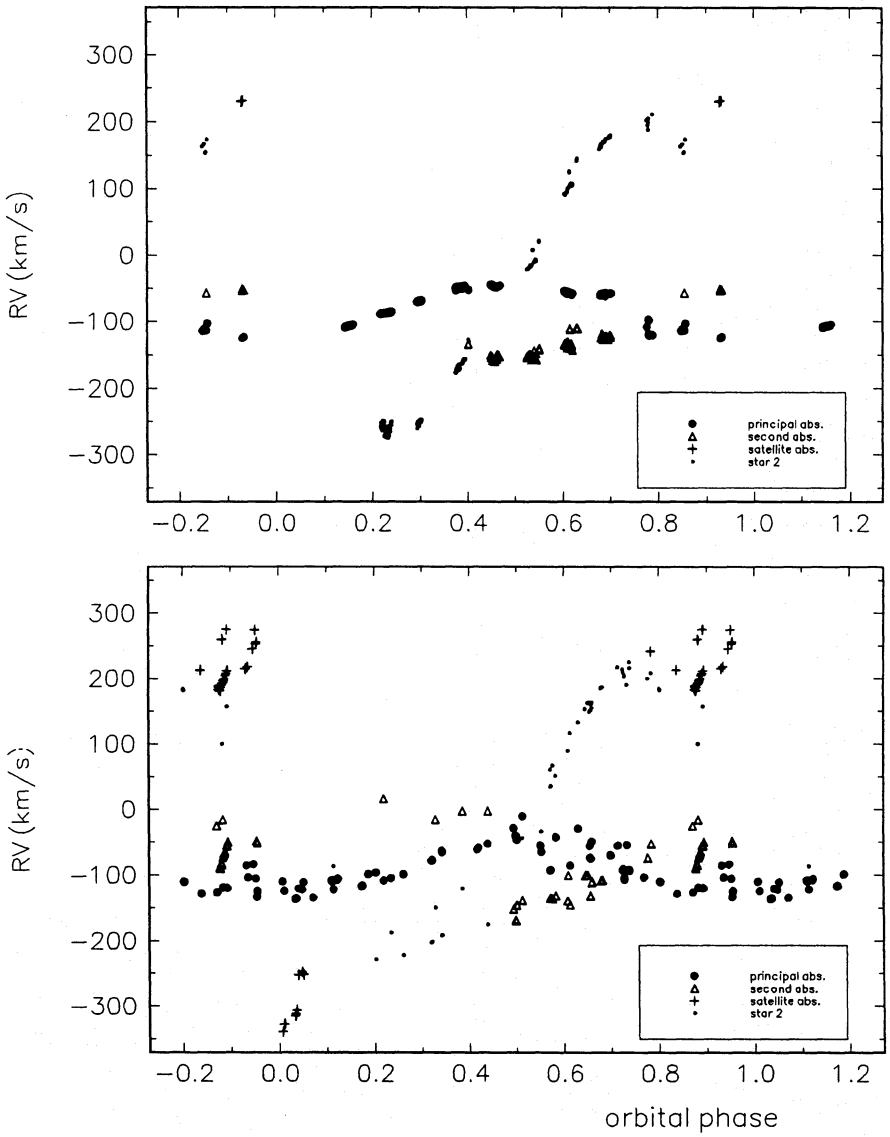

Fig. 10. Orbital RV curves of all distinct absorption features measured in the He I 6678 line profiles. *Upper panel:* CCD spectra; *Bottom panel:* Reticon spectra. Note that the RV curve of the principal absorption component, denoted by filled circles, closely corresponds to that of Hα.

used the 1994 light curve in the R band, which characterizes the continuum variations in the wavelength region covered by interferometric and spectral observations.

We estimated the peak intensities of the Hα emission at the binary elongations and minima. At both elongations (phases $0^P.25$ and $0^P.75$), the peak intensities are similar, about 2.52–2.54. The measured peak intensities at the primary minimum for cycles 3195–3196 were:

4.423 for cycle 3195.034 and 3.823 for cycle 3195.954.

Similar figures for the secondary minimum are

2.646 at 3194.493 and 2.866 at 3196.498.

If one assumes that the true emission power at Hα does not vary with the orbital phase, then the apparent emission-peak intensity variations with phase should correspond only to the fact that the emission is normalized to varying continuum corresponding to the R light curve. This, however, would imply peak intensities of 5.88 and 3.89 at the primary and the secondary minimum, respectively, much higher than actually observed. This may indicate that a part of the emission originates from a region located between both stars and is, therefore, partly eclipsed at both minima.

Fig. 11 shows the V-band light curve (in relative intensities) for all V observations at our disposal. A good agreement with the ephemeris by Harmanec & Scholz (1993) is once more found. To characterize the general shape of the mean light curve, and to investigate systematically the non-orbital light variations reported by several authors, we calculated a Fourier fit of the light curve. To overcome the problem of the secularly increasing orbital period of β Lyr, we used the calculated orbital phases instead of Julian dates of the observations as the independent variable in the fit. This way, we could simply fit frequency 1 c d^{-1} and its harmonics in the phase space. After some trials, we found that the best fit, giving the lowest rms error per one observation of 0.0302, was obtained for seven frequencies

1, 2, 3, 4, 5, 6, and 9 c d^{-1},

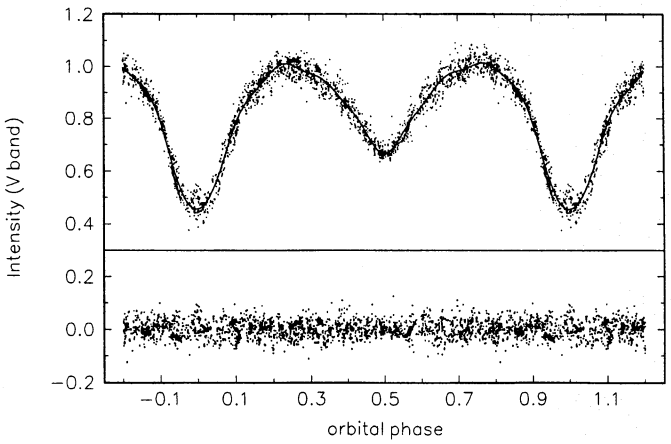

Fig. 11. The V-band intensity orbital light curve of β Lyr, based on all 2852 observations available to us, which cover an interval of 36 yrs. A Fourier fit to the data is shown by the solid line (see the text for details of the fit). The bottom panel shows the O-C deviations from the fit.

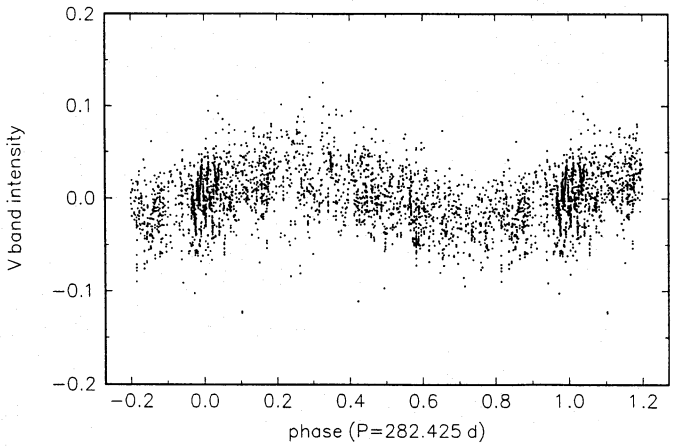

Fig. 12. All V-band intensity residuals from the orbital light curve of β Lyr plotted vs. phase of the best-fit period of $282^{d}.425$. An arbitrary epoch HJD 2400000 was chosen in this and following plots as phase zero.

contribution of all other harmonic terms having amplitudes well below $0^{m}.01$. As another test, we also split the observations into two subsets in time, having similar lengths. The above seven-frequency fit to both subsets led to remarkably similar amplitudes and phases for both these fits. *In this sense*, we therefore confirm the conclusion by Wilson (1974) that the *mean* light curve of β Lyr *is* secularly quite stable. However, the scatter of the O-C deviations from the mean light curve appears larger than what is expected from the photometric accuracy of the data. The mean rms errors of the check star 9 Lyr in relative intensities from individual stations range from 0.004 to 0.025.

Note that the Fourier fit to the mean light curve indicates that both minima have broad shoulders with slopes strongly differing from those of the minima themselves. One is even tempted to say that β Lyr has not the typical β Lyr-type light curve.

5. Non-orbital spectral and light variations

5.1. The 280-d cycle

5.1.1. V-band residuals from the orbital light curve

We run a period search in the V-intensity residuals from the mean light curve (cf. the bottom panel of Fig. 11) over the range from 10 to 5000 d, using Stellingwerf's (1978) phase dispersion minimalization method. A period of about 282 d was found as the most significant one. We also tested several subsets of data: observations obtained relative to HR 6997 only (none of these was used by Van Hamme et al. 1995), and the first and second half of the data (with JD 2444000 as the boundary). Periods in the range 270–290 d were detected in all of them.

We then calculated a least-squares fit of the formula $f(t) = A \sin(2\pi P^{-1}(t - T_0))$ to all V-intensity residuals. This resulted in:

$P = 282^{d}.425 \pm 0^{d}.070$, $A = 0.0236 \pm 0.0008$,
T_0 = HJD 2446835.1 $\pm$1.4, and
rms of 1 observation of 0.0266.

The corresponding phase plot is shown in Fig. 12. The above values are to be compared to the result by Van Hamme et al. (1995):

$P = 283^{d}.39 \pm 0^{d}.26$ and T_0 = HJD 2446840.1 $\pm$7.7.

It is seen that while both epochs agree within the limits of their errors, the values of the period seem to differ.

We note that Van Hamme et al. (1995) were also recovering the values of the period shorter than 283 d from most of their individual subsets of data and preferred the value of 283.4 d in an effort to preserve secular coherence in phase. However, one can have some doubts about the legitimity of recovering a less than 5 % change from *visual* estimates, at least without a very careful discussion of associated errors. As seen in Fig. 6 of Van Hamme et al., 9 months was a rather typical length of the season of Baxendell's visual observations. During each season, the star goes from one horizon to the other one, changing inevitably its apparent colour with the zenith distance. This must cause a small systematic effect in the visual observations. A large indeterminacy in the value of the 282-d period also follows from the fact that even for our photoelectric data the semiamplitude of the variation is smaller than the associated rms error per 1 observation, and this ratio is much less favourable for visual data.

Considering that the sine fit of V residuals with the 282-d period decreased the rms error per one observation from 0.030 to 0.027 only, and inspecting the time plots of the residuals presented by Van Hamme et al. (1995), we even suspect that the 282-d change may be cyclic rather than strictly periodic.

To investigate the problem further, we created subsets of our V data from various parts of the orbital light curve, grouped in $0^{P}.1$ bins in orbital phase and with a step $0^{P}.05$ in orbital phase. We found that the 282-d periodicity almost disappears (and is not formally detected as the best one) near two orbital phases, $0^{P}.25$ and $0^{P}.50$. We therefore re-derived the value of the 282-d period fitting only data from orbital phases $0^{P}.60$ to $0^{P}.15$. This gave a marginally shorter value of the period, $282^{d}.370 \pm 0^{d}.081$, with

a larger semiamplitude of 0.0277 but with the rms of 0.0271, a bit worse than before.

Then we calculated sine fits to individual phase bins, keeping the period fixed at $282^{d}.370$, to investigate the variation of the amplitude A, zero epoch T_0 and scatter (rms) with the orbital phase. The $282^{d}.37$-phase curves for several selected phase bins are shown in Fig. 13. One can see that there are indeed very significant variations in the amplitude of the 282-d cycle with the orbital phase. The variation almost disappears at phases $0^{P}.25$ and $0^{P}.50$ and has the largest amplitude at phase $0^{P}.05$ where the putative gas stream between the stars re-appears projected against the visible disk of star 2 after the primary mid-eclipse. Also the epoch of zero phase and the scatter of the residuals seem to vary systematically with the orbital phase. The lowest scatter is observed at phases $0^{P}.05$ and $0^{P}.50$ while it is largest around phase $0^{P}.65$ where we also found the largest scatter in the Hα and He I 6678 absorption RVs.

Period analyses in the data from individual phase bins detected periods near 282 d in all subsets but those centred on orbital phases $0^{P}.20$, $0^{P}.30$, $0^{P}.50$ and $0^{P}.95$ where a yet longer period of about 1200 – 1240 d was detected. (This periodicity was reported in some spectroscopic studies in the past.)

In passing we note that the long period is near to resonance with the orbital one:

$22 \times 12^{d}.9346 = 284^{d}.56$.

Should there be a direct relation between the orbital period and the 282-d cycle, a secular change of the value of the 282-d period, parallel to the orbital-period increase, could also occur.

All this indicates that the 280-d variation is somehow related to the structure of circumstellar matter in the vicinity of star 1 and represents an important piece of evidence about the system geometry, to be fully explored in the future.

5.1.2. Spectral variations

We tested the residuals of absorption and emission Hα and He I 6678 RVs from the orbital solutions for the presence of the 282-d periodicity. It seems that there is no such indication in the absorption velocities which seem to be dominated by more rapid changes (see below). One may suspect the presence of the 282-d modulation in the emission RVs. The direct evidence is weak but if the presence of a sinusoidal 282-d variation with a semiamplitude of about 15 km s^{-1} is postulated, the systemic velocity of the residual emission RVs gets very close to the systemic velocity of the binary system (while it was for some 20 km s^{-1} too positive after the orbital solution only).

5.2. Rapid spectral variations

Fig. 14 shows the He I 6678 line profiles from different orbital cycles for four selected narrow phase intervals for which we have good time coverage. Amazing cycle-to-cycle variations are seen at first sight. Inspection of this figure (and other profiles at our disposal) reveals that these non-orbital variations occur on a time scale *shorter than one orbital period.* This result is in a good accord with a similar finding made by Olsen & Etzel (1995)

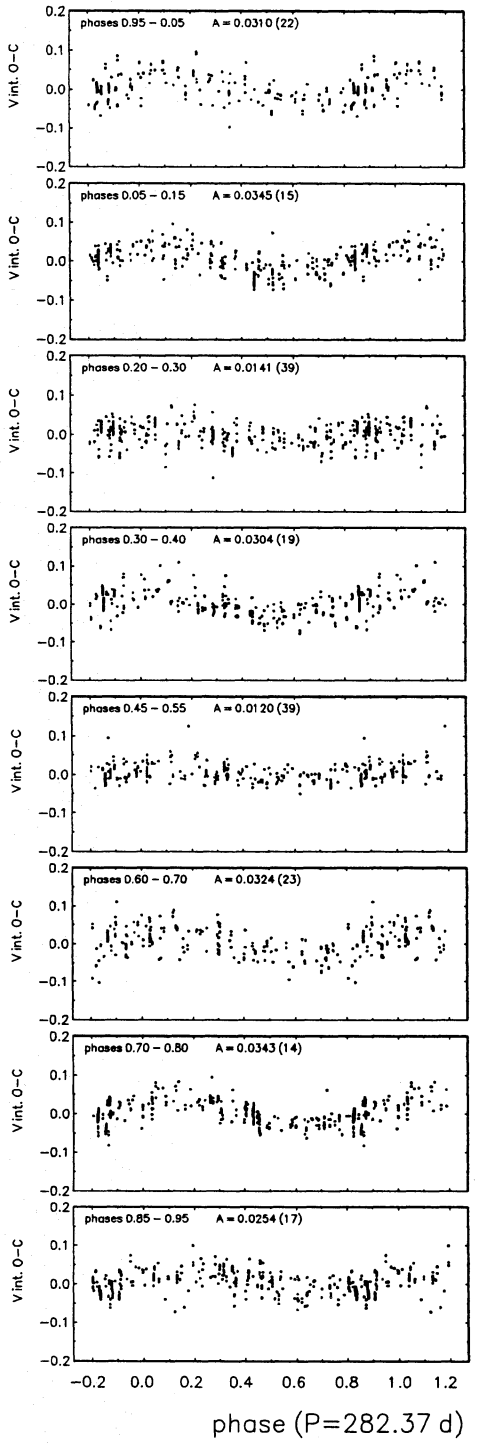

Fig. 13. The 282.370-d phase curves shown for various subsets of V-intensity residuals selected in $0^{P}.1$ wide bins for different orbital phases of β Lyr. It illustrates how the amplitude, phase and scatter for the 282.37-d period vary with the orbital phase. The semi-amplitude A and its rms error are given for each orbital-phase bin shown

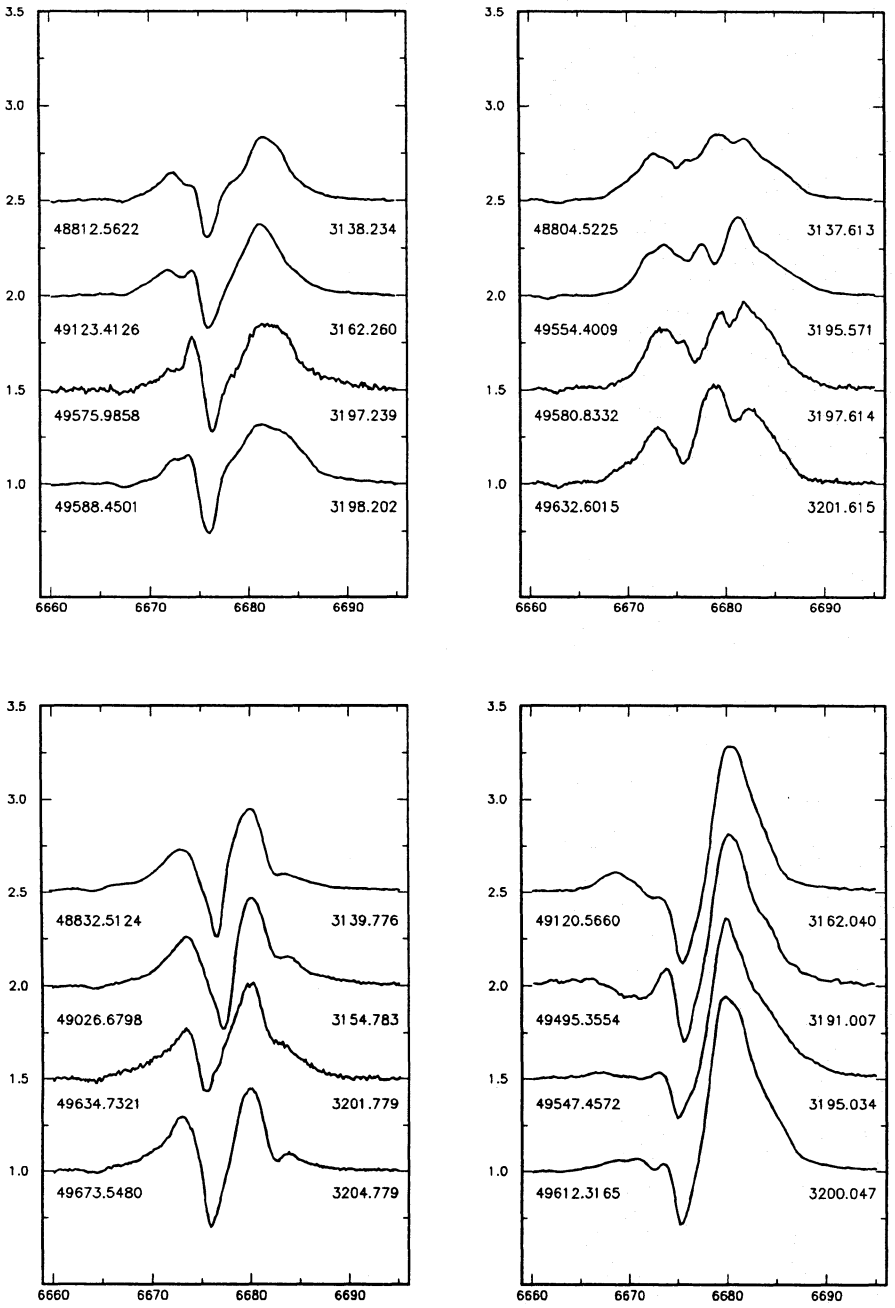

Fig. 14. A selection of He I 6678 line profiles of β Lyr from different orbital cycles compared in four narrow phase intervals. Very pronounced variations on a time scale shorter than one orbital period are evident. Heliocentric Julian dates minus 240000, cycle numbers and phases are given for each profile

for 9 other emission-line eclipsing binaries. However, our conclusion is that at least a part of these variations is caused by changing *absorption* part of the profiles.

A closer inspection of Fig. 14 shows that the variations are not completely chaotic. Rather, one gets the impression that various absorption components disappear and re-appear at defined wavelenths which agrees with the fact that we were able to define RV curves for several distinct absorption features. In other words, there may be a rather stable geometric structure and the variations are due to rapid changes in absorbing power at given location.

Naturally, we also tried to search for a short period which would reconcile the rapid changes. We found that the data for both emission- and absorption-RV residuals for both lines can best be reconciled with a number of periods near 4.70 – 4.75 d (several close aliases are possible due to data spacing). For illustration, we have chosen one of these periods which seems to reconcile the data well: 4.731403 d — see Fig. 15 — but stress that the exact value cannot be derived uniquely at the moment. It is also true that this periodicity is mainly defined by the excellent DAO series of observations which span an interval of 100 d in 1994. These are, however, the most accurate RV data at our disposal because of their good dispersion and resolution. In 1994, the orbital period of β Lyr was $12^{\mathrm{d}}.9385$ and we note that

$$3 \times (12.9385^{-1} - 2 \times 282.425^{-1}) = 4.7479^{-1}.$$

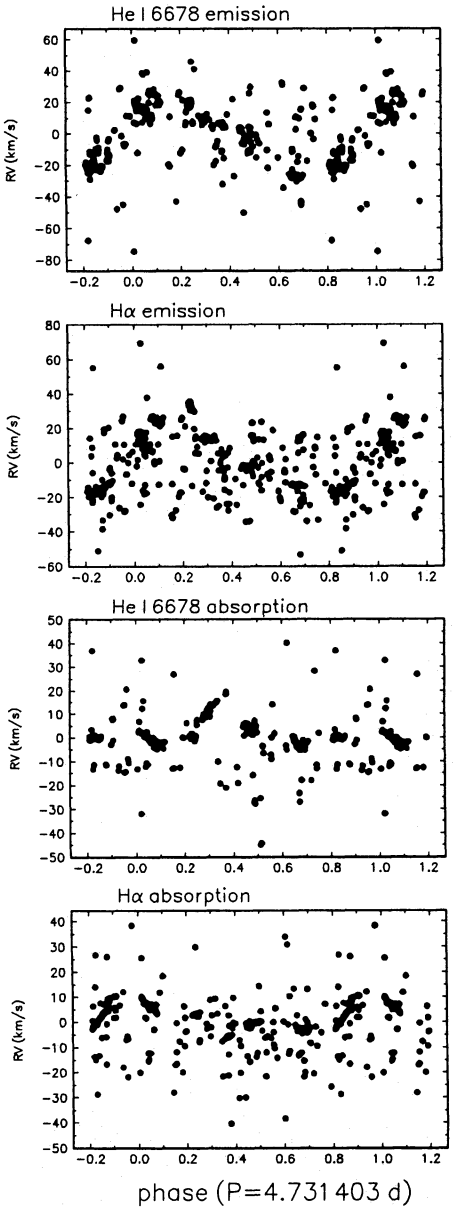

Fig. 15. The O-C deviations of the Hα and He I 6678 emission-wings and absorption-core RVs from the formal orbital solutions quoted above vs. phase of the 4.731403-d period. The presence of this periodicity seems to be mainly defined by the systematic DAO series of observations which span an interval of 100 d. They are, at the same time, the most accurate RV mausurements at our disposal.

This may indicate a causal relationship between the long period, seen in photometry, and rapid spectral changes.

6. Toward a new model of β Lyr

The current picture of β Lyr is that the system is in an advanced, yet quite rapid phase of mass transfer from star 2 toward star 1. Star 1 is believed to be largely hidden inside a huge accretion disk which is optically thick even in continuum and re-radiates the light of star 1 away from the orbital plane. Most of the authors also believe that the mass transfer is non-conservative with part of material leaving the system altogether. Blue-shifted optical (He I in particular) and many UV absorption lines were considered to evidence such an outflow.

Harmanec (1992) pointed out a serious problem with this picture: A dynamical outflow of gaseous matter from the binary via the Lagrangian point L_2 would lead to the creation of a circumbinary envelope in the form of an outflowing spiral (as first demonstrated by Kuiper 1941). Therefore, the bulk of the outflowing material, responsible for the blue-shifted absorption lines, would remain concentrated near the orbital plane of the binary. However, the continuum flux of β Lyr in the orbital plane consists of a combination of the radiation from the B6-8II star and the disk rim ($T_{\rm eff} \sim 8000$ K). This radiation is *unable* to excite spectral lines corresponding to effective temperatures over 20000 K. Harmanec (1992) therefore concluded that the blue-shifted lines must originate above the polar regions of star 1, possibly in the form of 'bipolar jets' of material perpendicular to the orbital plane.

Here, we argue that the new findings presented in this paper can indeed be best reconciled if the current geometrical model of β Lyr (involving the accretion disk and the gas stream between the stars) is complemented by jet-like structures associated with star 1 and its circumstellar environment. Let us discuss the relevant arguments in turn.

6.1. Interferometry

As already mentioned, the exciting thing about the interferometric findings is that *the source appears to be always more extended in the V than in the R peak, independent of the orbital phase* (see Fig. 4). This is a very unexpected behaviour since any bright structure near the equatorial plane of the binary, revolving with the system as the binary moves in orbit, should manifest itself by the cyclic variations of the visibility ratio as it would either recede from, or approach to the observer.

A plausible explanation is that the bulk of the Hα emission is formed in 'jets' of gaseous material which are perpendicular to the orbital plane of the binary and expand. Since the part of the 'jet' which moves away from us is partly hidden from view by the disk around star 1 (recall the binary-orbit inclination of 83°), it is always the blue portion of the jet (i.e. the V peak of the emission) which appears more extended.

This conjecture is also supported by the fact that the region producing the Hα emission as a whole appears more extended than the separation of binary components and cannot, therefore, be fully identified with the material within the Roche lobe around star 1.

Future interferometric observations could help to confirm the above picture. If the bulk of the Hα emission comes from side lobes of a 'jet' of gas expanding along the North-South direction, then a wavelength-dependent variation of the phase of the complex visibility function across the Hα line should be observed. To the first order, this phase contains positional information about the blue and red components of the jet and could be used

to the determination of their north-south orientation with respect to the orbital plane of the binary (Vakili, Mourard & Stee 1994).

6.2. *Spectroscopy and photometry*

6.2.1. Hα and He I 6678 absorption

The position of the region responsible for these absorptions, derived from the observed phase-locked RV variations, agrees well with the expected position of a hot spot formed as a result of interaction of the gas stream flowing from star 2 toward star 1 with the inner dense parts of the accretion disk. Obviously, the stream penetrates through the less dense outer parts of the disk — cf., e.g., Šíma & Hadrava (1987). At the same time, one is led to the conclusion that the true seat of the absorption is absorption and self-absorption in one of the 'jets', that one which is above the 'visible face' of the disk and intersect it at the above estimated position of the 'hot spot'. The absorption cannot originate in the 'spot' only since the latter is hidden from view in many orbital phases by the disk around star 1 as well as by star 2. Given the high rate of the mass transfer (implied by the fast increase of the orbital period), it is conceivable that the dense inner parts of the disk (at a disk radius of about 11 $R_\odot$) represent a 'solid wall' for the infalling stream and deflect it (at least partly) to flow away from the orbital plane and to form the jets.

The observed systemic velocity of the Hα and He I 6678 absorptions is for about 65 km s^{-1} more negative than the systemic velocity of the binary system. This indicates a steady outflow of the absorbing material. If this outflow proceeds along the 'jet', i.e. along a direction perpendicular to the orbital plane, the true outflow velocity is −533 km s^{-1} for the adopted inclination of the binary orbit. Typical RVs of the observed optical blue-shifted lines range from −100 to −200 km s^{-1}. If they also originate in one of the jets, this would imply their true outflow velocities of about −800 to −1600 km s^{-1}. *These are velocities comparable to the wind velocities of hot stars.*

We also call attention to the observed disappearance of the sharp Hα absorption soon after orbital phase $0^P.5$ which agrees with the idea that the parts of the 'jet' which are closer to the orbital plane are eclipsed by star 2.

Finally, note the similarity of the absorption parts of some profiles from the two opposite elongations of the binary, cf. profiles from cycles 3162.260 and 3201.779 in Fig. 14. This is not expected for a line arising from the neighbourhood of a hot spot only.

6.2.2. Hα and He I 6678 emissions

The analysis of the phase-locked RV variations of the Hα and He I 6678 emission lines indicated that the 'optical centre' of these emissions is quite close to the centre of star 1, only slightly shifted towards the position of the putative hot spot.

It is also interesting to note that both emission peaks of the Hα emission are observed at velocities of about ±150 km s^{-1} (cf. Fig. 9). This compares very well with the *absorption* velocities of the optical blue-shifted lines — in accordance with the idea that the bulk of these emission lines is formed in the jets. Note that if the peak separation of the double Hα emission would be interpreted as due to Keplerian rotation (as for other Be stars), the corresponding effective radius of the emission region would be more than 100 $R_\odot$ — *well outside* the Roche lobe around star 1 (which has a radius of about 30 $R_\odot$). The same is also true for the Hβ emission profiles published by several authors. This is in clear contradiction with our finding that the material responsible for the Balmer emission moves in orbit with the binary. Note that Mazzali et al. (1992) concluded that also the broad UV emission lines are too broad to originate in the disk around star 1.

We stress, however, that some contribution to the emission obviously comes from the disk, both from its outer parts and from inner parts above the disk 'face' seen thanks to the fact that the orbital inclination differs from 90°. The third contribution to the emission is the gas stream and hot spot. This follows from the RV curve and from the peak-intensity variations related to the R-band light curve: a part of the emission is obviously eclipsed during both eclipses.

6.3. *Polarimetric evidence*

While finishing this study, we received a copy of a report by Nordsieck et al. (1995) on the first preliminary results of spectropolarimetry of β Lyr obtained during the Astro-2 mission in March 1995 and simultaneous optical observations. They found a sharp intrinsic polarization change of 90° at 3750 Å which they also independently interpreted as signature of bipolar jets in β Lyr.

6.4. *The 282.5-d cycle*

The fact that the variations related to this long cycle almost disappear at orbital phases $0^P.25$ and $0^P.50$ seems to point toward association of the seat of these changes with some part of the circumstellar matter associated with star 1. Note that the scatter of V data at the elongation is large which may indicate the effect of the gas stream and hot spot while the scatter is very low — comparable to photometric accuracy — when star 1 is eclipsed. We do not think we can specify the true physical reason of the 282.5-d variation at the moment. We note, however, that it is reminiscent of the 164-d light modulation, found in addition to the 13.074-d binary-orbit modulation for V1343 Aql = SS433, the archetype of the binary systems with bipolar jets — cf., e.g., Kemp et al. (1981).

6.5. *General remarks*

Concluding, we stress that the arguments presented in this first step of the analysis define the new component of the circumstellar matter, the bipolar jets, mainly in the geometrical sense. At the moment, we do not make any firm statements about the physical nature of the jets. It is quite likely that they should be identified with the strong stellar wind, collimated by the 'shielding effect' of the huge accretion disk (and perhaps the

gas stream) but the possibility that they are jets similar to those known for yet more exotic objects also cannot be excluded.

One notable thing of a more general importance is that within our new interpretation we see no need to postulate an outflow of matter via the Lagrangian point L_2 from the binary system, and see no observational evidence of it.

Acknowledgements. PHar. gratefully acknowledges the support from CNRS which allowed him to work one month at Plateau de Calern station of the Observatoire de la Côte d'Azur and organize the observational program reported here. He also thanks all the colleagues and staff there for their warm hospitality during his stay. The study was completed during a visit of DB and DM to Ondřejov which benefited of the support of the Groupe de Recherche "milieux circumstellaires" from CNRS. The research of YJ, SY, and GAHW was supported by a research grant from the Natural Sciences and Engineering Research Council of Canada to GAHW. CS acknowledges a research grant from the Belgian Fund for Scientific Research (NFWO). Our thanks are due to Drs. J. Horn, P. Koubský, J. Kubát, V. Šimon, P. Škoda, S. Štefl, and M. Wolf who at our request obtained some of the Ondřejov spectrograms of β Lyr, and to Mr. Tom Sterken for assistance during the photolectric observations at Jungfraujoch. Dr. A.H.Batten very kindly communicated the exact dates of mid-exposures for the Hα spectrograms investigated by Batten & Sahade (1973). We are also very obliged to Dr. M.S. Sonntag who kindly put a preprint of his study, and his individual BV observations at our disposal prior to publication. Thanks are due to Dr. Nordsieck who generously informed us about the spectropolarimetric results prior to publication and sent us a copy of a poster paper by him and his colleagues dealing with UV and optical spectropolarimetry of β Lyr. We greatly benefited from detailed constructive comments on the first version of this paper by Drs. C. Tom Bolton and Ivan Hubeny. Finally, an anonymous referee convinced us to re-think some parts of the text and make it more compact.

References

Abt H.A., Jeffers H.M., Gibson J., Sandage A.R. 1962, ApJ 135, 429
Alekseev G.N., Skulskij M.Yu. 1989, Astrofiz. Issledovaniya, Izv. SAO 28, 21
Appenzeller I. and Hiltner W. A. 1967 ApJ 149, 353
Aslan Z., Derman E., Engin S., Yilmaz N. 1987, A& AS 71, 597
Batten A.H., Sahade J. 1973, PASP 85, 599 and priv.com.
Berghöfer T.W., Schmitt J.H.M.M. 1994, A & A 292, L5
Blackwell D.E., Shallis M. J. 1977, MNRAS 180, 177
Blazit A. 1987, PhD, Univ. of Nice
Boyd L.J., Genet R.M., Hall D.S., Busby M.R., Henry G.W. 1990, IAPPP Com. 42, 54-57
Burnashev V.I., Skulskij M.Yu. 1980, Pisma AZh 6, 587 = Sov. Astron. Lett. 6, 307
Burnashev V.I., Skulskij M.Yu. 1991 Izv. Krym 83, 108
De Greve J.P., Linnell A.P. 1994, A & A 291, 786
Dobias J.J., Plavec M.J. 1985, AJ 90, 773
Flora U., Hack M. 1975, A& AS 19, 57
Guinan E.F. 1989, Space Sci. Rev. 50, 35
Hadrava P. 1990, Contr.Astron.Obs.Skalnaté Pleso 20, 23
Hadrava P. 1995, *FOTEL3 User's guide*, rel. Oct. 16, 1995, Astronomical Institute, Academy of Sciences, Ondřejov, anonymous ftp 147.231.24.100, file pub/fotel/fotel3.tex
Harmanec P. 1990, A & A 237, 91
Harmanec P. 1992, A & A 266, 307
Harmanec P., Horn J. 1995 *Manual (rel. 3) and a package of FORTRAN programs for photometric data reduction, archiving, sorting and retrieval*, Ondřejov Observatory, Be Star Newsletter No. 30, 24
Harmanec P., Scholz G. 1993, A & A 279, 131
Harmanec P., Horn J., Juza K. 1994, A& AS 104, 121
Hubeny I., Plavec M.J. 1991, AJ 102, 1156
Hubeny I., Harmanec P., Shore S.N. 1994, A & A 289, 411
Jameson R. F. and King A. R. 1978 A & A 63, 285
Kemp J.C., Barbour M.S., Kemp G.N., Hagood D.M. 1981, Vistas in Astronomy 25, 31
Kříž S. 1974, Bull. Astron. Inst. Czechosl. 25, 6
Kuiper G.P. 1941, ApJ 93, 133
Landis H.J., Lovell L.P., Hall D.S. 1973 PASP 85, 133
Larsson-Leander G. 1970, Vistas in Astronomy 12, 183
Leggett S.K., Mountain C.M., Selby M.J., Blackwell D.E., Booth A.J., Haddock D.J., Petford A.D. 1986, A & A 159, 217
Leone F. Trigilio C. and Umana G. 1994 A & A 283, 908
Lovell L.P., Hall D.S. 1970 PASP 82, 345 UBV
Lovell L.P., Hall D.S. 1971 PASP 83, 357 UBV
Mazzali P.A., Pauldrach A.W.A., Puls J., Plavec M.J. 1992, A & A 254, 241
McLean I. S. 1977 A & A 55, 347
Mourard D., Bonneau D., Blazit A., Labeyrie A., Morand F., Percheron I., Tallon-Bosc I., Vakili F. 1992, in *Complementary Approaches to Double and Multiple Star Research*, IAU Col. 135, ASP Conf. Ser. 32, 510
Mourard D., Tallon-Bosc I., Blazit A., Bonneau D., Merlin G., Morand F., Vakili F., Labeyrie A. 1994a, A & A 283, 705
Mourard D., Tallon-Bosc I., Rigal F., Vakili F., Bonneau D., Morand F., Stee Ph. 1994b, A & A 288, 675
Nordsieck K.H., Fox G.K., Code A.D., Anderson C.M., Babler B.L., Bjorkman K.S., Edgar R.J., Johnson J.J., Lupie O.L., Meade M.R. et al. 1995, *UV/Visible Spectropolarimetry of Interacting Binaries by WUPPE and University of Wisconsin Pine Bluff Observatory*, a poster paper presented at the American Astronomical Society Meeting at Pittsburgh, USA, June 13, 1995
Olsen E.C., Etzel P.B. 1995, AJ 109, 1308
Plavec M.J. 1985, in *Interacting Binaries*, eds. P.P. Eggleton and J.E. Pringle, Reidel, Dordrecht, 155
Rudy J.R. 1979, MNRAS 186, 473
Sahade J. 1980, Space Sci. Rev. 26, 349
Šíma Z., Hadrava P. 1987, Ap& SS 130, 151
Skulskij M. Yu. 1972, Izv. Krym. Astrophys. Obs. 55, 135
Skulskij M. Yu. 1992, Pisma AZh 18, 711
Skulskij M. Yu. 1993a, Pisma AZh 19, 114
Skulskij M. Yu. 1993b, Pisma AZh 19, 417
Skulskij M. Yu., Malkov Yu.F. 1992, AZh 69, 291
Skulskij M. Yu., Topilskaya G.P. 1991, Pisma AZh 17, 619
Sonntag M.S. 1995, IAPPP Communications No. 61, 56
Stellingwerf R.F. 1978, ApJ 224, 953
Thiebaut E. 1994, A & A 284, 340
Vakili F., Mourard D., Stee P. 1994, in *Pulsation, Rotation and Mass Loss in Early-Type Stars*, IAU Symp. 162, Ed. by L.A. Balona, H.F. Henrichs and J.-M. Le Contel, Kluwer, Dordrecht, 435
Van Hamme W., Wilson R.E., Guinan E.F. 1995, AJ 110, 1350
Wilson R.E. 1974, ApJ, 189, 319
Wilson R.E., Terrell D. 1992, Ann. New York Acad. Sci. Vol. 675, 65
Wood D.B., Walker M.F. 1960 ApJ 131, 363
Wood D.B. 1973 ApJ 186, 615